HHS Public Access

Author manuscript

DNA Repair (Amst). Author manuscript; available in PMC 2021 December 01.

Published in final edited form as:

DNA Repair (Amst). 2020 December ; 96: 102977. doi:10.1016/j.dnarep.2020.102977.

Treatment of human cells with 5-aza-dC induces formation of PARP1-DNA covalent adducts at genomic regions targeted by DNMT1

Kostantin Kiianitsa[1], **Yinbo Zhang**[1], **Nancy Maizels**[1,2,*]

[1]Department of Immunology, University of Washington, Seattle, WA 98195 USA

[2]Department of Biochemistry, University of Washington, Seattle, WA 98195 USA

Abstract

The nucleoside analog 5-aza-2'-deoxycytidine (5-aza-dC) is used to treat some hematopoietic malignancies. The mechanism of cell killing depends upon DNMT1, but is otherwise not clearly defined. Here we show that PARP1 forms covalent DNA adducts in human lymphoblast or fibroblasts treated with 5-aza-dC. Some adducts recovered from 5-aza-dC-treated cells have undergone cleavage by apoptotic caspases 3/7. Mapping of PARP1-DNA adducts, by a new method, "Adduct-Seq", demonstrates adduct enrichment at CpG-dense genomic locations that are targets of maintenance methylation by DNMT1. Covalent protein-DNA adducts can arrest replication and induce apoptosis, and these results raise the possibility that induction of PARP1-DNA adducts may contribute to cell killing in response to treatment with 5-aza-dC.

Keywords

DNA-protein crosslink; DNA methylation; 5-methylcytosine; CG island; decitabine; RADAR enrichment

1. Introduction

The nucleoside analog 5-aza-2'-deoxycytidine (5-aza-dC; clinically known as decitabine) is incorporated opposite G during DNA replication. Incorporation of 5-aza-dC opposite 5-methyl-CpG creates a target for methylation by the maintenance DNA methyltransferase,

*correspondence: maizels@uw.edu.

CRediT author statement:

Kostantin Kiianitsa: Conceptualization, Methodology, Investigation, Visualization; Writing - Original Draft; Writing - Review & Editing

Yinbo Zhang: Investigation, Methodology, Validation, Visualization, Writing - Review & Editing

Nancy Maizels: Conceptualization, Methodology, Visualization, Writing - Original Draft, Writing - Review & Editing, Funding acquisition, Project administration

Conflict of interest statement

The authors declare that there is no conflict of interest regarding the publication of this article.

DNMT1. Treatment of mammalian cells with 5-aza-dC also causes proteolysis of DNMT1 that results in genomewide loss of cytosine methylation and extensive epigenetic reprogramming [1–3]]. This gave rise to the notion that 5-aza-dC might re-activate silenced tumor suppressor genes to limit cell proliferation, and 5-aza-dC is used in the clinic as an "epigenetic drug" to treat myelodysplasia syndrome (MDS) and acute myelogenous leukemia (AML) in patients who are unlikely to tolerate other treatments [4]. However efforts to demonstrate that 5-aza-dC efficacy correlates with reprogramming of specific genetic networks or pathways have not been fruitful [5]. This prompted us to further investigate the possibility that cell killing results from DNA damage induced by 5-aza-dC treatment.

DNMT1 normally forms an obligatory but transient covalent bond with its target in the course of transfer of a methyl group from S-adenosyl methionine to DNA [6, 7]. Perturbation of normal resolution of DNMT1-DNA adducts at 5-aza-substituted sites can contribute to cytotoxicity. Diminished 5-aza-dC sensitivity upon DNMT1 depletion [8, 9] and correlation of drug sensitivity with expression level of DNMT1 protein [3] are consistent with a DNMT1-dependent mechanism being a principal source of cytotoxicity. Treatment with 5-aza-dC results in DNA damage evident as characteristic point mutations in surviving cells [8, 10] and strand breaks and genomic rearrangements [9, 11–13]. Abasic (AP) sites have been shown to accumulate in 5-aza-dC-treated cells [14] in experiments that used an aldehyde-reactive probe [15] for their direct detection. AP site induction has also been inferred from experiments that demonstrate APE1 involvement in repair of 5-aza-dC-induced damage, by the use of methoxyamine to poison AP sites to prevent their further processing by APE1 [14] and by the use of low doses of APE1 inhibitor III to increase the cytotoxic efficacy of 5-aza-dC [16].

PARP1 is a conserved and abundant factor involved in repair and transcriptional regulation which is recruited to many kinds of damage, including base damage like that resulting from 5-aza-dC treatment [14, 17–20]. PARP1 has been shown to form covalent adducts with DNA substrates containing AP sites or 5'-dRP residues in vitro, and in living cells treated with an alkylating agent [21–23]. Persistent covalent protein-DNA adducts can cause replication arrest and induce apoptosis. This led us to hypothesize that recruitment of PARP1 to damage resulting from aberrant DNMT1 activity at 5-aza-substituted cytosines might cause PARP1-DNA adducts to form and then persist, arresting replication and inducing apoptosis.

To test this, we have isolated PARP1-DNA adducts from human cells treated with 5-aza-dC and characterized adducted PARP1 by Western blotting and adducted DNA by genomic sequencing. Here we report that PARP1-DNA adducts can be readily recovered from 5-aza-dC treated cells. Caspase cleavage of PARP1 is a hallmark of apoptosis [24–26], and some PARP1 adducts carried the signature N-terminal neo-epitope generated upon caspase cleavage. Adducted DNA fragments were sequenced using a new method, "Adduct-Seq", which demonstrated highly significant enrichment at genomic features characteristic of the CpG islands (CGIs) that are targets of methylation by DNMT1. Caspase-cleaved PARP1 is impaired for recruitment to chromatin [27], and while we cannot rule out the possibility that caspase cleavage of PARP1 occurred prior to adduct formation, our results better support a

model in which aberrant activity of DNMT1 at 5-aza-substituted regions creates damage that recruits PARP1 to form covalent adducts, which arrest replication and kill cells.

2. Materials and Methods

2.1 Cells, cell culture, siRNA depletion and drug treatment

K562 lymphoblasts (ATCC CCL-243) were obtained from ATCC and cultured in RPMI medium with 10% fetal calf serum. GM639 cells (gift of Dr. Ray Monnat, University of Washington), were cultured in DMEM medium with 10% fetal calf serum. 5-aza-dC was obtained from Calbiochem/EMD Millipore; the PARP inhibitor BMN-673 (talazoparib), from ApexBio; and the topoisomerase 1 inhibitor topotecan from Enzo Life Sciences. Ambion Silencer® Select Validated siRNA to TP53 (#4427038, siRNA ID: s605) and Negative Control No. 2 siRNA (siNT2, #4390846) were purchased from Thermo Fisher. siRNA transfection of GM639 cells was performed using Lipofectamine RNAiMax (Invitrogen) according to the manufacturer's protocol.

2.2 Antibodies

Antibodies used for Western blots included: anti-rec-PARP1, a rabbit polyclonal raised against recombinant PARP1 (Enzo Life Sciences ALX-210–302-R100; 1:4000 dilution); anti-N-ter-PARP1, a rabbit polyclonal raised against the N-terminal half of recombinant PARP1 (Active Motif Ab 2793257, 1:2000 dilution); anti-C-ter-PARP1, an affinity-purified mouse mAb that recognizes an epitope in the C-terminal NAD binding and catalytic domain of human PARP1 (clone 7D3–6, BD Biosciences #556493; 1:500 dilution); anti-cc-PARP1, a mouse mAb specific for the neo-epitope generated at the N-terminal of the 89 kD PARP1 fragment formed after cleavage by apoptotic caspases between Asp214/Gly215 (clone F21–852, BD Biosciences #552596, 1:1000 dilution). Secondary detection was with HRP-conjugated goat anti-mouse IgG or donkey anti-rabbit IgG (BioLegend, #405306 and #406401, respectively; 1:5000 dilution). Immune complexes were visualized using the SuperSignal West system (Pierce). Specificity of PARP1 Abs for full-length 113 kD PARP1 and its cleavage products was assessed by Western blots of whole cell extracts treated with staurosporine (EMD Millipore; 1 μM, 1 hr), a kinase inhibitor that induces apoptotic PARP1 cleavage (Fig. S1A).

2.3 Flow cytometry

Approximately 1×10^6 cells were harvested by either pipetting (K562) or trypsinization (0.05%; GMG39) then washed twice with cold PBS. Samples were resuspended in 200 μl PBS and analyzed by flow cytometry on a BD LSR II instrument, set to record 50,000 cells per sample. Linear area of width and height of the forward scatter (FSC) and side scatter (SSC) were recorded. To assay viability by dye exclusion, cells were stained in 250 μl of Fixable Viability Dye eFluor™ 450 (Invitrogen™; 1:1000 dilution in PBS) for 15 min on ice, then washed prior to resuspension and flow cytometry. To detect cells containing caspase-cleaved PARP1, cells were fixed and permeabilized with 500 μl of 1x Foxp3 / Transcription Factor Fixation/Permeabilization solution (Invitrogen™) for 30 min at room temperature; washed twice with 500 μl of 1x Foxp3/Transcription Factor permeabilization buffer (Invitrogen); stained with 250 μl of PE-conjugated anti-cc-PARP1 in the same buffer

(#552933, BD Biosciences; 1:100 dilution) for one hr at room temperature; washed once in 1 ml; and resuspended in 200 μl for flow cytometry. Data were analyzed using FlowJo software (version 9.6). The linear area of FSC and SSC were gated relative to untreated cells to represent the relative cell size and internal complexity. Fluorescent channel Pacific Blue was collected in log area to measure cells labeled with viability dye (dead cells), and fractions of dead cells were gated by using the histogram of log area of positive Pacific Blue signal of the untreated whole cell population, compared to the histogram of unstained cells. Fluorescent channel PE was collected in log area to measure cells labeled with PE-conjugated anti-cc-PARP. Fractions of cells containing cleaved PARP1 were gated by PE positive among SSC, using unstained cells as a reference.

2.4 Nucleic acid and protein quantification

DNA and RNA were quantified using DNA/RNA specific fluorescent detection kits (Qubit, Invitrogen). Total protein was measured using BCA detection kit (Pierce).

2.5 RADAR/Western analysis

DNA-protein adducts were purified for RADAR/Western analysis using an adaptation of the RADAR (Rapid Approach to DNA Adduct Recovery) fractionation protocol in which cells or nuclei are directly lysed in the presence of chaotrope and detergents, after which nucleic acids including protein-DNA adducts are separated from total protein by precipitation in alcohol [28, 29]. Preparations used 2–3 × 10^7 K562 cells or 1.5–2.5 × 10^7 GM639 cells. Cells were harvested by centrifugation and washed in PBS. Cytoplasm, including rRNA and up to 75% of total protein was eliminated by quick lysis in 1 ml MPER reagent (Pierce/Thermo Fisher) supplemented with Halt protease inhibitor cocktail (Thermo Fisher) and 1 mM DTT. Homogenization was performed by 8–10 pipet strokes, then nuclear pellets collected by 2 min centrifugation at maximal speed. PARP1 and DNMT1 were confirmed to be exclusively in the pellet by Western blotting; as was essentially all genomic DNA. Pellets were promptly lysed in 400 μl of RADAR lysis buffer (LS1), consisting of 5 M guanidinium isothiocyanate (GTC), 2% Sarkosyl, 10 mg/ml DTT, 20 mM EDTA, 20 mM Tris-HCl (pH 8.0) and 0.1 M sodium acetate (pH 5.3), and adjusted to final pH 6.5 with NaOH. Lysates were transferred to polystyrene tubes (Evergreen) and sonicated on ice using a cup horn device (QSONICA) with ten 30 sec pulses at amplitude 100, and 60 sec cool-off time between pulses. Sonication yielded an average DNA size of 500 bp. After sonication, lysates were mixed with 80 μl 12 M LiCl (final concentration 2M LiCl, 4.16 M GTC) and incubated for 10 min at 37°C on a Thermoshaker, then cleared by 10 min centrifugation at 14,000 rpm at room temperature prior to conservative recovery of the supernatant. Lysates (volume approximately 450 μl) were transferred to new tubes, mixed with an equal volume of isopropanol; and nucleic acids were precipitated by 5 min centrifugation at 14,000 rpm at room temperature. Pellets were washed thrice with 1 ml 75% ethanol, followed by 2 min centrifugation. Nucleic acid pellets were dissolved in 100–200 μl of freshly prepared 8 mM NaOH by 30–60 min shaking on a Thermomixer at 37°C; then neutralized by addition of 1 M HEPES to a final concentration of 20 mM. The resulting samples contained mostly genomic DNA and some nuclear RNA, with a yield of approximately 70 μg DNA per 10^7 cells. The DNA/protein weight ratio was 100:3 or higher, comparable to adducts prepared by ultracentrifugation in a CsCl gradient [30].

Prior to gel electrophoresis, samples containing 10–30 μg genomic DNA were treated with Benzonase nuclease (EMD Millipore; 0.5 units per μg DNA) in the presence of 2 mM magnesium chloride for 30 min at 37°C to digest DNA. Completeness of nuclease digestion was verified by Qubit assays. Samples were resolved on precast 4–12% gradient protein gels (Bolt, Invitrogen), transferred to nitrocellulose membranes (0.45 μM pore, Invitrogen) and probed with antibodies in PBST buffer (PBS containing 0.05% Tween 20) with 0.5% alkali-soluble casein (Novagen) as blocking agent.

2.6 Adduct-Seq analysis

To identify genomic locations of adducted PARP1, we developed an approach, "Adduct-Seq" which resembles ChIP-Seq but depends upon adduction rather than formaldehyde-induced crosslinking to form stable protein-DNA complexes. An analogous approach has previously been used to enrich genomic DNA adducted to Topoisomerase 1 [31]. In brief, adducts were first isolated from approximately 1.5×10^7 untreated or treated cells by RADAR fractionation, sonicated as above to reduce the size of adducted DNA; PARP1-DNA adducts captured by anti-PARP1 mAbs bound to a solid support; and adducted DNA fragments released by Proteinase K treatment and sequenced. To avoid melting of duplex DNA that may later interfere with adaptor ligation for Illumina sequencing, DNA was resuspended with 5 mM tris-HCl (pH 8.5) rather than 8 N NaOH. Antibody capture was performed using a ChromaFlash High-Sensitivity ChIP kit (Epigentek) according to the manufacturer's instructions. Briefly, strip wells were pre-coated with anti-C-ter-PARP1 mAb (see above; 800 ng IgG per well), unbound mAbs removed by washing, then incubated with 40 μg RADAR-fractionated DNA overnight at 4°C in 100 μl of provided buffer, washed, treated with RNase A and rewashed. DNA was released by treatment with Proteinase K and purified using a ChIP DNA Clean & Concentrator kit (Zymo Research). DNA yield was approximately 1– 2 ng/10^7 cells, and 1.5 ng DNA was subject to paired end Illumina sequencing, 100 nt per read, with ~40 million read pairs per sample sequencing depths.

Raw reads were mapped to human genome (hg38) using Bowtie2. Genomic locations (peaks) of adducted PARP1 in response to treatment were identified by MACS2 from mapped reads of Adduct-Seq libraries ("narrow peak" calling option, $p<0.01$ cutoff) using the untreated sample to assess background. The GenometriCorr R package (https://doi.org/10.1371/journal.pcbi.1002529 [32]) was used to test spatial correlation of PARP1 peaks and 31,144 CGIs available as standard track on the UCSC Genome Browser. Multiple tests were performed to assess spatial correlation: absolute and relative distance between query (PARP1 peaks) and reference (CGIs), Jaccard test (union vs intersection for each reference feature) and projection test (overlap of query with reference features). GC fraction and CpG density of query and reference sequences were calculated using R functions gcContent and cpgDensity, respectively.

2.7 Statistical analyses

Graphing, calculation of mean values and statistical tests of significance were performed using GraphPad Prism software.

3. Results

3.1 TP53 contributes to synthetic lethality in combined treatment with 5-aza-dC and PARPi

While treatment with 5-aza-dC is typically restricted to myeloid malignancies, there is interest in extending its use to other contexts by combining it with other drugs. Several small molecule inhibitors of PARP1 catalytic activity are currently FDA-approved treatments for some kinds of solid tumors [33, 34]; and in some contexts combined treatment with 5-aza-dC and PARPi has a synthetic lethal effect, although with considerable variability among cell types tested [14, 17]. As a first step toward testing the possibility that PARP1 forms DNA adducts in response to 5-aza-dC treatment, we therefore characterized the response of two different human cell lines to treatment with 5-aza-dC or PARPi alone and in combination. Dose-response analyses showed that K562 cells [35], an extensively studied p53-null ENCODE cell line derived from a chronic myelogenous leukemia patient in blast crisis, was sensitive to 5-aza-dC and to PARPi as single agents, but no more sensitive to 5-aza-dC+PARPi combined (Fig. 1A). GM639 cells, derived from human skin fibroblasts immortalized by SV40 [36], were less sensitive than K562 cells to 5-aza-dC or PARPi (BMN-673 (known in the clinic as talazoparib) alone, but very sensitive to both drugs together (Fig. 1A). Treatment with 5-aza-dC resulted in rapid degradation of DNMT1 and induction of the apoptotic 89 kD PARP1 fragment in both K562 and GM639 cells (Fig. S1B), as documented for other mammalian cell types [3]. Further differences between these two cell types were evident by flow cytometric analysis of forward and side scatter, where GM639 but not K562 cells treated with both drugs exhibited robust treatment time-dependent changes in cell size and morphology (Fig. S2A) and faster progression to apoptosis, as evidenced by appearance of double caspase 3/7 cPARP1 positive cells (Fig. S2B).

The distinct survival and apoptotic responses of K562 and GM639 cells to the combined effects of 5-aza-dC+PARPi suggested that drug synergy might reflect the status of genes that control the fate of drug-treated cells. A key regulator of this process is p53 protein, an essential tumor suppressor that controls cell division and initiation of apoptosis in response to genome damage [37]. In K562 cells, p53 protein is completely absent due to loss of one allele of the TP53 gene and an inactivating mutation in the other [38]. In contrast, some p53 activity may remain in SV40-immortalized GM639 cells, where functional inactivation of p53 protein by binding to SV40 T antigen may be influenced by the balance of expression or activity of these two proteins [39]. To test whether residual p53 protein in GM639 cells might affect drug sensitivity or synergy, TP53 was depleted by siRNA treatment. TP53 depletion did not affect sensitivity to 5-aza-dC but caused a modest increase in resistance of GM639 cells to PARPi and a dramatic increase in resistance to PARPi combined with 5-aza-dC (Fig. 1B). Similarly, TP53 depletion was also protective against the potent topoisomerase 1 poison, topotecan (Fig. S2C); and others have reported that TP53 contributes to synthetic lethality of PARPi and ionizing radiation [40], suggesting that this effect is not treatment-specific but may reflect the importance of p53 protein in regulating apoptotic cell death.

3.2 RADAR/Western blots identify PARP1-DNA adducts induced by 5-aza-dC

The 113 kD PARP1 polypeptide (Fig. 2A) contains an N-terminal DNA binding domain (DBD) and a C-terminal domain that catalyzes polymerization of poly(ADP-ribose) (PAR) from the coenzyme, NAD^+, enabling PARP1 to modify itself and other proteins by addition of chains of PAR ("PARylation") which stimulates protein recruitment for DNA repair. In apoptotic cells, activated caspases 3/7 cleave 113 kD PARP1 at Asp214 within the DBD to generate fragments of 24 and 89 kD, creating a neo-epitope that is a hallmark of apoptosis. This made it important to not only establish whether PARP1-DNA adducts had formed but also to address the possibility that adducts had been cleaved by apoptotic caspases. To do so, K562 or GM639 cells were treated with 1 μM 5-aza-dC or 1 μM PARPi; or pretreated with for 48 hr with 5-aza-dC, allowing time for its incorporation into newly replicated DNA, after which PARPi was added and culture continued. Next nuclei were isolated and adducts recovered out using a modification of the RADAR extraction method developed in our laboratory, in which cells or nuclei are treated with a combination of chaotropic salts and detergent to disrupt non-covalent protein-DNA interactions, and then nucleic acids, including covalent DNA-protein complexes, precipitated with alcohol [28–30]. Finally, recovered proteins were resolved by Western blots and probed with antibodies tested for recognition of full-length PARP1 and its apoptotic fragments (Fig. 2A).

Probing adducts recovered from K562 cells with anti-recombinant PARP1 (anti-rec-PARP1, Enzo) identified species of 89 kD and smaller (55–65 kD) in samples treated with 5-aza-dC (66 hr) or treated with 5-aza-dC prior to treated with PARPi; but not in samples treated with PARPi alone (Fig. 2B, left). Reprobing this same blot with anti-N-ter-PARP1, which recognizes full-length PARP1 and both the 24 kD and 89 kD products of caspase cleavage, showed that samples treated with 5-aza-dC alone contained 113 kD PARP1-DNA adducts as well as larger PARP1 species that appear to be PARylated, as they were not evident in cells treated with PARPi, which inhibits PARylation (Fig. 2B, right). The anti-N-ter-PARP1 antibody also identified adducted 113 kD PARP1 and smaller species in extracts of cells treated with PARPi alone (18 hr).

Adducts recovered from GM639 fibroblasts treated with 5-aza-dC, PARPi, or 5-aza-dC +PARPi were analyzed by duplicate RADAR/Western blots run in parallel and probed with either anti-C-ter-PARP1, which recognizes both full-length and caspase-cleaved PARP1; or anti-cc-PARP1, which specifically recognizes the apoptotic N-terminal neo-epitope of caspase-cleaved PARP1. These two mAbs produced nearly identical staining patterns (Fig. 2C). In samples from cells treated with 5-aza-dC alone or 5-aza-dC+PARPi, both mAbs identified 89 kD cleaved PARP1 and smaller species (45–65 kD). Detection with anti-cc-PARP1 mAb, which specifically recognizes the apoptotic N-terminal neo-epitope, identifies the smaller species (45–65 kD) as probable proteolysis products of the adducted apoptotic 89 kD fragment. Comparably faint staining was evident in samples from untreated cells and cells treated with PARPi.

The results of RADAR/Western blots thus confirm the hypothesis that PARP1 forms covalent DNA adducts in cells treated with 5-aza-dC.

3.2 Mapping genomewide locations of covalent protein-DNA adducts by Adduct-Seq

If 5-aza-dC treatment causes PARP1-DNA adducts to form at hemi-methylated CpG dinucleotides that are targets of DNMT1 (Fig. 3A, left), then adducted DNA will be enriched in CGI, about half of which are associated with elevated DNA methylation [41–44]. CGI in human cells are defined by high GC fraction (>50%) and enrichment of CpG dinucleotides (http://genome.ucsc.edu/cgi-bin/hgTrackUi?g=cpgIslandExt) and by spatial position. These features are readily quantified by genomic sequencing.

In order to recover adducted genomic DNA fragments suitable for sequencing, we developed an approach, “Adduct-Seq”, that relies solely on endogenous covalent DNA-protein crosslinks to recover protein-bound DNA (Fig. 3A, right). RADAR extracts were prepared as for ChiP-Seq, but without addition of formaldehyde or other exogenous treatments to induce protein-DNA adduct formation. Samples were sonicated to reduce DNA length, then PARP1 and covalently bound PARP1-DNA adducts were captured by anti-C-ter-PARP1 mAb bound to a solid surface. Following deproteinization, recovered DNA was analyzed by genomic sequencing.

Samples were prepared from K562 or GM639 cells, untreated or treated with 5-aza-dC, PARPi, or 5-aza-dC+PARPi. From each sample of 1.5×10^7 cells, 1.5–2.3 ng of PARP1-adducted DNA was recovered. Sequencing on an Illumina platform generated from 4.5–5.0 $\times 10^7$ mapped reads per sample (Fig. 3B). Samples from untreated cells were used to identify and assess background interactions and thereby distinguish the effects of drug treatment from intrinsic affinity of PARP1 for specific genomic regions. The untreated sample thus provides a control for background analogous to the “Input” sample in ChIP-Seq.

3.3 Adduct-Seq demonstrates PARP1-DNA adduct enrichment at CGI

Analysis of nucleotide composition of sequenced libraries (Fig. 4A) showed that the GC fraction of untreated samples was 42.0 (K562) and 42.5% (GM639), very close to the 41% average of the human genome. The GC fractions of adducts recovered from K562 cells treated with 5-aza-dC or 5-aza-dC+PARPi were significantly greater than that average (45.5% and 43.8% respectively; $p<0.0001$, Mann-Whitney test); while the GC fraction of adducts recovered from cells treated with PARPi alone was slightly lower than that average (39.7%). The GC fractions of adducts recovered from GM639 cells treated with 5-aza-dC or 5-aza-dC+PARPi were also significantly above the genomic average (47.2%, and 52.1%, $p<0.0001$, Mann-Whitney test), with the latter exceeding the 50% threshold defined for human CGI; while the GC fraction of adducts recovered from GM639 cells treated with PARPi alone (42.7%) was comparable to the genomic average.

Mean CpG densities of adducted DNA were determined (Fig. 4B) and compared to the human genome, where average CpG density is close to 0.01 and reaches 0.19 in CGIs. Mean CpG densities of adducted DNA recovered from K562 cells treated with 5-aza-dC or 5-aza-dC+PARPi were similar (0.030 and 0.028, respectively), significantly greater than either the genomic average or mean CpG density of adducts recovered from cells treated with PARPi alone (0.018; $p<0.0001$, two-tailed Mann-Whitney test). Mean CpG densities of adducted DNA recovered from GM639 cells treated with 5-aza-dC, PARPi or 5-aza-dC+PARPi were

all significantly greater than the genomic average (0.041, 0.029, and 0.060 respectively; $p<0.0001$, two-tailed Mann-Whitney test).

Analysis of spatial correlation (Fig. 4C–D) of PARP1 peaks and the 31,144 CGIs in the human genome (CGI track in the UCSC Genome Browser) identified highly significant proximity and overlap among adducts recovered from K562 lymphoblasts treated with 5-aza-dC (relative distance test p=3.6e-12, projection test p=0). Significant proximity to CGI also characterized adducts recovered from K562 cells treated with 5-aza-dC+PARPi (p=0.003); but not adducts recovered from K562 cells treated with PARPi alone (p=0.2). Among adducts recovered from GM639 fibroblasts, highly significant proximity and overlap with CGI was observed in samples treated with either single agent 5-aza-dC or PARPi (relative distance test p=4.6e-12 and 0, projection test p=0 and 0, respectively), and combined treatment with both 5-aza-dC and PARPi further shifted adduct location towards CGI.

Adduct-Seq thus demonstrates that PARP1-adducted DNA fragments isolated from 5-aza-dC-treated K562 and GM639 cells exhibit significant enrichment for genomic features characteristic of targets of DNMT1 methylation: elevated GC fraction and CpG density and spatial overlap with CGI (Fig. 4). Genomewide analysis thus supports the hypothesis that PARP1 forms covalent adducts at sites of DNMT1 activity in 5-aza-dC-treated cells.

4. Discussion

The results reported here identify a plausible mechanistic pathway for cell killing by 5-aza-dC. Fig. 5 outlines a simple working model for this pathway. In the course of normal replication, 5-aza-dC is incorporated opposite 5-me-CpG. DNMT1 is recruited to methylate the newly incorporated base, but the 5-aza group renders this a suicide substrate. Repair results in DNA damage, which recruits PARP1. Evidence for accumulation of AP sites and involvement of APE1 in repair in 5-aza-dC-treated cells [14, 16] suggests a potential role for abasic site/dRP-mediated PARP1 crosslinking at sites of adduct formation, but our results do not exclude crosslinking to other kinds of DNA lesions. Adducted PARP1 can block replication, which will in turn activate apoptotic caspases 3/7 to cleave adducted PARP1.

The model specifically postulates that PARP1-DNA adducts form at the damage created by 5-aza-dC at hemi-methylated CpG dinucleotides that are targets for DNMT1. This was established by Adduct-Seq analysis (Fig. 3) of PARP1-adducted DNA fragments isolated from 5-aza-dC treated K562 and GM639 cells. Adducted fragments exhibit genomic features consistent with enrichment for targets of DNMT1 methylation: significantly elevated GC fraction and CpG density, and significant spatial overlap with CGI (Fig. 4). These results support a model in which aberrant activity of DNMT1 at 5-aza-substituted regions creates damage that recruits PARP1 to form covalent adducts, which arrest replication and induce apoptosis, activating caspase 3/7 cleavage of PARP1 (Fig. 5). Caspase cleavage generates the hallmark neo-epitope readily detected by RADAR-Western blots (Fig. 2), and caspase-cleaved PARP1 is disabled for critical activities including DNA damage recognition and DNA damage dependent PAR synthesis, and particularly chromatin recruitment [25–27, 45, 46]. While we cannot rule out the possibility that PARP1 was cleaved by apoptotic caspases

prior to adduct formation, our results better support a model in which aberrant activity of DNMT1 at 5-aza-substituted regions creates damage that recruits PARP1 to form covalent adducts, which arrest replication and induce apoptosis.

The model for cell killing by PARP1-DNA adducts outlined here (Fig. 5) is supported by experimental analysis of both the myeloid line, K562; and the fibroblast line, GM639. Details of the response of these two lines is different, particularly the resistance of K562 cells to synergistic killing of 5-aza-dC+PARPi evident in GM639 cells (Fig. 1A) and the extensive accumulation of adducts in CGI in GM639 cells (Fig. 4C, D). The p53 tumor suppressor protein contributes to drug synergy (Fig. 1B), which may be informative when identifying specific contexts in which combination drug treatment may be informative. Mechanisms that may determine localization of adduct formation may be influenced by a number of mechanisms, among them transcription, local modifications of histones and non-histone chromosomal proteins, chromosomal domain organization, and early vs. late replication. Further studies are necessary to address this interesting question.

The results reported here suggest the importance of revisiting the commonly held view of 5-aza-dC as an “epigenetic drug” [4, 5]. While treatment with 5-aza-dC undoubtedly affects genomewide methylation, induction of covalent adducts that block replication represents a straightforward path to cell killing that deserves further investigation. The results reported here further suggest that PARP1-DNA adducts may contribute to cell killing not only by 5-aza-dC, but also to other drugs, including PARPi, which can be readily tested by Adduct-Seq. If so, this may open the way to new therapeutic opportunities and combinations.

Supplementary Material

Refer to Web version on PubMed Central for supplementary material.

Acknowledgments

This research was supported by the US NIH National Cancer Institute (R01 CA183967 and P01 CA077852 to N.M.). We are grateful to Feinan Wu at the Fred Hutch, Seattle for assistance in analysis of Adduct-Seq results; and to Dr. Rajendra Prasad, National Institute of Environmental Health Sciences, for advising us on the antibodies for PARP1 adduct analyses.

References

[1]. Ghoshal K, Datta J, Majumder S, Bai S, Kutay H, Motiwala T, Jacob ST, 5-Aza-deoxycytidine induces selective degradation of DNA methyltransferase 1 by a proteasomal pathway that requires the KEN box, bromo-adjacent homology domain, and nuclear localization signal, Mol Cell Biol, 25 (2005) 4727–4741.Epub.10.1128/MCB.25.11.4727-4741.2005. [PubMed: 15899874]

[2]. Patel K, Dickson J, Din S, Macleod K, Jodrell D, Ramsahoye B, Targeting of 5-aza-2’deoxycytidine residues by chromatin-associated DNMT1 induces proteasomal degradation of the free enzyme, Nucleic Acids Res, 38 (2010) 4313–4324.Epub.10.1093/nar/gkq187. [PubMed: 20348135]

[3]. Yu J, Qin B, Moyer AM, Nowsheen S, Liu T, Qin S, Zhuang Y, Liu D, Lu SW, Kalari KR, Visscher DW, Copland JA, McLaughlin SA, Moreno-Aspitia A, Northfelt DW, Gray RJ, Lou Z, Suman VJ, Weinshilboum R, Boughey JC, Goetz MP, Wang L, DNA methyltransferase expression in triple-negative breast cancer predicts sensitivity to decitabine, J Clin Invest, 128 (2018) 2376–2388.Epub.10.1172/JCI97924. [PubMed: 29708513]

[4]. Estey EH, Epigenetics in clinical practice: the examples of azacitidine and decitabine in myelodysplasia and acute myeloid leukemia, Leukemia, 27 (2013) 1803–1812.Epub.10.1038/leu.2013.173. [PubMed: 23757301]

[5]. Klco JM, Spencer DH, Lamprecht TL, Sarkaria SM, Wylie T, Magrini V, Hundal J, Walker J, Varghese N, Erdmann-Gilmore P, Lichti CF, Meyer MR, Townsend RR, Wilson RK, Mardis ER, Ley TJ, Genomic impact of transient low-dose decitabine treatment on primary AML cells, Blood, 121 (2013) 1633–1643.Epub.10.1182/blood-2012–09-459313. [PubMed: 23297133]

[6]. Gros C, Fahy J, Halby L, Dufau I, Erdmann A, Gregoire JM, Ausseil F, Vispe S, Arimondo PB, DNA methylation inhibitors in cancer: recent and future approaches, Biochimie, 94 (2012) 2280–2296.Epub.S0300–9084(12)00307–0 [pii] 10.1016/j.biochi.2012.07.025. [PubMed: 22967704]

[7]. Miletic V, Odorcic I, Nikolic P, Svedruzic ZM, In silico design of the first DNA-independent mechanism-based inhibitor of mammalian DNA methyltransferase Dnmt1, PLoS One, 12 (2017) e0174410Epub.10.1371/journal.pone.0174410. [PubMed: 28399172]

[8]. Juttermann R, Li E, Jaenisch R, Toxicity of 5-aza-2'-deoxycytidine to mammalian cells is mediated primarily by covalent trapping of DNA methyltransferase rather than DNA demethylation, Proc Natl Acad Sci U S A, 91 (1994) 11797–11801.Epub. [PubMed: 7527544]

[9]. Maslov AY, Lee M, Gundry M, Gravina S, Strogonova N, Tazearslan C, Bendebury A, Suh Y, Vijg J, 5-aza-2'-deoxycytidine-induced genome rearrangements are mediated by DNMT1, Oncogene, 31 (2012) 5172–5179.Epub.10.1038/onc.2012.9. [PubMed: 22349820]

[10]. Jackson-Grusby L, Laird PW, Magge SN, Moeller BJ, Jaenisch R, Mutagenicity of 5-aza-2'-deoxycytidine is mediated by the mammalian DNA methyltransferase, Proc Natl Acad Sci U S A, 94 (1997) 4681–4685.Epub. [PubMed: 9114051]

[11]. Palii SS, Van Emburgh BO, Sankpal UT, Brown KD, Robertson KD, DNA methylation inhibitor 5-Aza-2'-deoxycytidine induces reversible genome-wide DNA damage that is distinctly influenced by DNA methyltransferases 1 and 3B, Mol Cell Biol, 28 (2008) 752–771.Epub.10.1128/MCB.01799–07. [PubMed: 17991895]

[12]. Orta ML, Calderon-Montano JM, Dominguez I, Pastor N, Burgos-Moron E, Lopez-Lazaro M, Cortes F, Mateos S, Helleday T, 5-Aza-2'-deoxycytidine causes replication lesions that require Fanconi anemia-dependent homologous recombination for repair, Nucleic Acids Res, (2013).Epub.gkt270 [pii] 10.1093/nar/gkt270.

[13]. Burgos-Moron E, Calderon-Montano JM, Pastor N, Hoglund A, Ruiz-Castizo A, Dominguez I, Lopez-Lazaro M, Hajji N, Helleday T, Mateos S, Orta ML, The Cockayne syndrome protein B is involved in the repair of 5-AZA-2'-deoxycytidine-induced DNA lesions, Oncotarget, 9 (2018) 35069–35084.Epub.10.18632/oncotarget.26189. [PubMed: 30416680]

[14]. Orta ML, Hoglund A, Calderon-Montano JM, Dominguez I, Burgos-Moron E, Visnes T, Pastor N, Strom C, Lopez-lazaro M, Helleday T, The PARP inhibitor Olaparib disrupts base excision repair of 5-aza-2'-deoxycytidine lesions, Nucleic Acids Res, 42 (2014) 9108–9120.Epub.10.1093/nar/gku638. [PubMed: 25074383]

[15]. Viswesh V, Gates K, Sun D, Characterization of DNA damage induced by a natural product antitumor antibiotic leinamycin in human cancer cells, Chem Res Toxicol, 23 (2010) 99–107.Epub.10.1021/tx900301r. [PubMed: 20017514]

[16]. Kohl V, Flach J, Naumann N, Brendel S, Kleiner H, Weiss C, Seifarth W, Nowak D, Hofmann WK, Fabarius A, Popp HD, Antileukemic Efficacy in Vitro of Talazoparib and APE1 Inhibitor III Combined with Decitabine in Myeloid Malignancies, Cancers (Basel), 11 (2019).Epub.10.3390/cancers11101493.

[17]. Muvarak NE, Chowdhury K, Xia L, Robert C, Choi EY, Cai Y, Bellani M, Zou Y, Singh ZN, Duong VH, Rutherford T, Nagaria P, Bentzen SM, Seidman MM, Baer MR, Lapidus RG, Baylin SB, Rassool FV, Enhancing the Cytotoxic Effects of PARP Inhibitors with DNA Demethylating Agents - A Potential Therapy for Cancer, Cancer Cell, 30 (2016) 637–650. [PubMed: 27728808]

[18]. Hanzlikova H, Kalasova I, Demin AA, Pennicott LE, Cihlarova Z, Caldecott KW, The Importance of Poly(ADP-Ribose) Polymerase as a Sensor of Unligated Okazaki Fragments during DNA Replication, Mol Cell, 71 (2018) 319–331 e313.Epub.10.1016/j.molcel.2018.06.004. [PubMed: 29983321]

[19]. Zimmermann M, Murina O, Reijns MAM, Agathanggelou A, Challis R, Tarnauskaite Z, Muir M, Fluteau A, Aregger M, McEwan A, Yuan W, Clarke M, Lambros MB, Paneesha S, Moss P,

Chandrashekhar M, Angers S, Moffat J, Brunton VG, Hart T, de Bono J, Stankovic T, Jackson AP, Durocher D, CRISPR screens identify genomic ribonucleotides as a source of PARP-trapping lesions, Nature, 559 (2018) 285–289.Epub.10.1038/s41586–018-0291-z. [PubMed: 29973717]

[20]. Pascal JM, The comings and goings of PARP-1 in response to DNA damage, DNA Repair (Amst), 71 (2018) 177–182.Epub.10.1016/j.dnarep.2018.08.022. [PubMed: 30177435]

[21]. Khodyreva SN, Prasad R, Ilina ES, Sukhanova MV, Kutuzov MM, Liu Y, Hou EW, Wilson SH, Lavrik OI, Apurinic/apyrimidinic (AP) site recognition by the 5'-dRP/AP lyase in poly(ADP-ribose) polymerase-1 (PARP-1), Proc Natl Acad Sci U S A, 107 (2010) 22090–22095.Epub.10.1073/pnas.1009182107. [PubMed: 21127267]

[22]. Prasad R, Horton JK, Chastain PD, 2nd, N.R. Gassman, B.D. Freudenthal, E.W. Hou, S.H. Wilson, Suicidal cross-linking of PARP-1 to AP site intermediates in cells undergoing base excision repair, Nucleic Acids Res, 42 (2014) 6337–6351.Epub.10.1093/nar/gku288. [PubMed: 24771347]

[23]. Prasad R, Horton JK, Dai DP, Wilson SH, Repair pathway for PARP-1 DNA-protein crosslinks, DNA Repair (Amst), 73 (2019) 71–77.Epub.10.1016/j.dnarep.2018.11.004. [PubMed: 30466837]

[24]. Kaufmann SH, Desnoyers S, Ottaviano Y, Davidson NE, Poirier GG, Specific proteolytic cleavage of poly(ADP-ribose) polymerase: an early marker of chemotherapy-induced apoptosis, Cancer Res, 53 (1993) 3976–3985.Epub. [PubMed: 8358726]

[25]. Pascal JM, Ellenberger T, The rise and fall of poly(ADP-ribose): An enzymatic perspective, DNA Repair (Amst), 32 (2015) 10–16.Epub.10.1016/j.dnarep.2015.04.008. [PubMed: 25963443]

[26]. Cohen MS, Chang P, Insights into the biogenesis, function, and regulation of ADP-ribosylation, Nat Chem Biol, 14 (2018) 236–243.Epub.10.1038/nchembio.2568. [PubMed: 29443986]

[27]. Pettitt SJ, Krastev DB, Brandsma I, Drean A, Song F, Aleksandrov R, Harrell MI, Menon M, Brough R, Campbell J, Frankum J, Ranes M, Pemberton HN, Rafiq R, Fenwick K, Swain A, Guettler S, Lee JM, Swisher EM, Stoynov S, Yusa K, Ashworth A, Lord CJ, Genome-wide and high-density CRISPR-Cas9 screens identify point mutations in PARP1 causing PARP inhibitor resistance, Nat Commun, 9 (2018) 1849Epub.10.1038/s41467–018-03917–2. [PubMed: 29748565]

[28]. Kiianitsa K, Maizels N, A rapid and sensitive assay for DNA-protein covalent complexes in living cells, Nucleic Acids Res, 41 (2013) e104Epub.gkt171 [pii] 10.1093/nar/gkt171. [PubMed: 23519618]

[29]. Kiianitsa K, Maizels N, Ultrasensitive isolation, identification and quantification of DNA-protein adducts by ELISA-based RADAR assay, Nucleic Acids Res, (2014) In press.Epub.

[30]. Kiianitsa K, Maizels N, The "adductome": A limited repertoire of adducted proteins in human cells, DNA Repair (Amst), 89 (2020) 102825Epub.10.1016/j.dnarep.2020.102825. [PubMed: 32109764]

[31]. Husain A, Begum NA, Taniguchi T, Taniguchi H, Kobayashi M, Honjo T, Chromatin remodeller SMARCA4 recruits topoisomerase 1 and suppresses transcription-associated genomic instability, Nat Commun, 7 (2016) 10549Epub.10.1038/ncomms10549. [PubMed: 26842758]

[32]. Favorov A, Mularoni L, Cope LM, Medvedeva Y, Mironov AA, Makeev VJ, Wheelan SJ, Exploring massive, genome scale datasets with the GenometriCorr package, PLoS Comput Biol, 8 (2012) e1002529Epub.10.1371/journal.pcbi.1002529. [PubMed: 22693437]

[33]. D'Andrea AD, Mechanisms of PARP inhibitor sensitivity and resistance, DNA Repair (Amst), 71 (2018) 172–176.Epub.10.1016/j.dnarep.2018.08.021. [PubMed: 30177437]

[34]. Slade D, PARP and PARG inhibitors in cancer treatment, Genes Dev, 34 (2020) 360–394.Epub.10.1101/gad.334516.119. [PubMed: 32029455]

[35]. Lozzio CB, Lozzio BB, Human chronic myelogenous leukemia cell-line with positive Philadelphia chromosome, Blood, 45 (1975) 321–334.Epub. [PubMed: 163658]

[36]. Hwang SP, Kucherlapati R, Localization and organization of integrated simian virus 40 sequences in a human cell line, Virology, 105 (1980) 196–204.Epub.10.1016/0042–6822(80)90167–1. [PubMed: 6251605]

[37]. Aylon Y, Oren M, Living with p53, dying of p53, Cell, 130 (2007) 597–600.Epub.10.1016/j.cell.2007.08.005. [PubMed: 17719538]

[38]. Law JC, Ritke MK, Yalowich JC, Leder GH, Ferrell RE, Mutational inactivation of the p53 gene in the human erythroid leukemic K562 cell line, Leuk Res, 17 (1993) 1045–1050.Epub.10.1016/0145–2126(93)90161-d. [PubMed: 8246608]

[39]. Drayman N, Ben-Nun-Shaul O, Butin-Israeli V, Srivastava R, Rubinstein AM, Mock CS, Elyada E, Ben-Neriah Y, Lahav G, Oppenheim A, p53 elevation in human cells halt SV40 infection by inhibiting T-ag expression, Oncotarget, 7 (2016) 52643–52660.Epub.10.18632/oncotarget.10769. [PubMed: 27462916]

[40]. Sizemore ST, Mohammad R, Sizemore GM, Nowsheen S, Yu H, Ostrowski MC, Chakravarti A, Xia F, Synthetic Lethality of PARP Inhibition and Ionizing Radiation is p53-dependent, Mol Cancer Res, 16 (2018) 1092–1102.Epub.10.1158/1541–7786.MCR-18–0106. [PubMed: 29592899]

[41]. Illingworth RS, Gruenewald-Schneider U, Webb S, Kerr AR, James KD, Turner DJ, Smith C, Harrison DJ, Andrews R, Bird AP, Orphan CpG islands identify numerous conserved promoters in the mammalian genome, PLoS Genet, 6 (2010) e1001134Epub.10.1371/journal.pgen.1001134. [PubMed: 20885785]

[42]. Deaton AM, Bird A, CpG islands and the regulation of transcription, Genes Dev, 25 (2011) 1010–1022.Epub.10.1101/gad.2037511. [PubMed: 21576262]

[43]. Maunakea AK, Nagarajan RP, Bilenky M, Ballinger TJ, D'Souza C, Fouse SD, Johnson BE, Hong C, Nielsen C, Zhao Y, Turecki G, Delaney A, Varhol R, Thiessen N, Shchors K, Heine VM, Rowitch DH, Xing X, Fiore C, Schillebeeckx M, Jones SJ, Haussler D, Marra MA, Hirst M, Wang T, Costello JF, Conserved role of intragenic DNA methylation in regulating alternative promoters, Nature, 466 (2010) 253–257.Epub.10.1038/nature09165. [PubMed: 20613842]

[44]. Jeziorska DM, Murray RJS, De Gobbi M, Gaentzsch R, Garrick D, Ayyub H, Chen T, Li E, Telenius J, Lynch M, Graham B, Smith AJH, Lund JN, Hughes JR, Higgs DR, Tufarelli C, DNA methylation of intragenic CpG islands depends on their transcriptional activity during differentiation and disease, Proc Natl Acad Sci U S A, 114 (2017) E7526–E7535.Epub.10.1073/pnas.1703087114. [PubMed: 28827334]

[45]. Ray Chaudhuri A, Nussenzweig A, The multifaceted roles of PARP1 in DNA repair and chromatin remodelling, Nat Rev Mol Cell Biol, 18 (2017) 610–621.Epub.10.1038/nrm.2017.53. [PubMed: 28676700]

[46]. Alemasova EE, Lavrik OI, Poly(ADP-ribosyl)ation by PARP1: reaction mechanism and regulatory proteins, Nucleic Acids Res, 47 (2019) 3811–3827.Epub.10.1093/nar/gkz120. [PubMed: 30799503]

Highlights

- Elucidates a mechanism of cell killing by 5-aza-dC
- Presents a new method, Adduct-Seq, for mapping protein-DNA adducts genomewide
- Identifies targets and consequences of PARP1-DNA adduction in living cells
- Challenges the view of 5-aza-dC (decitabine) as an “epigenetic” drug

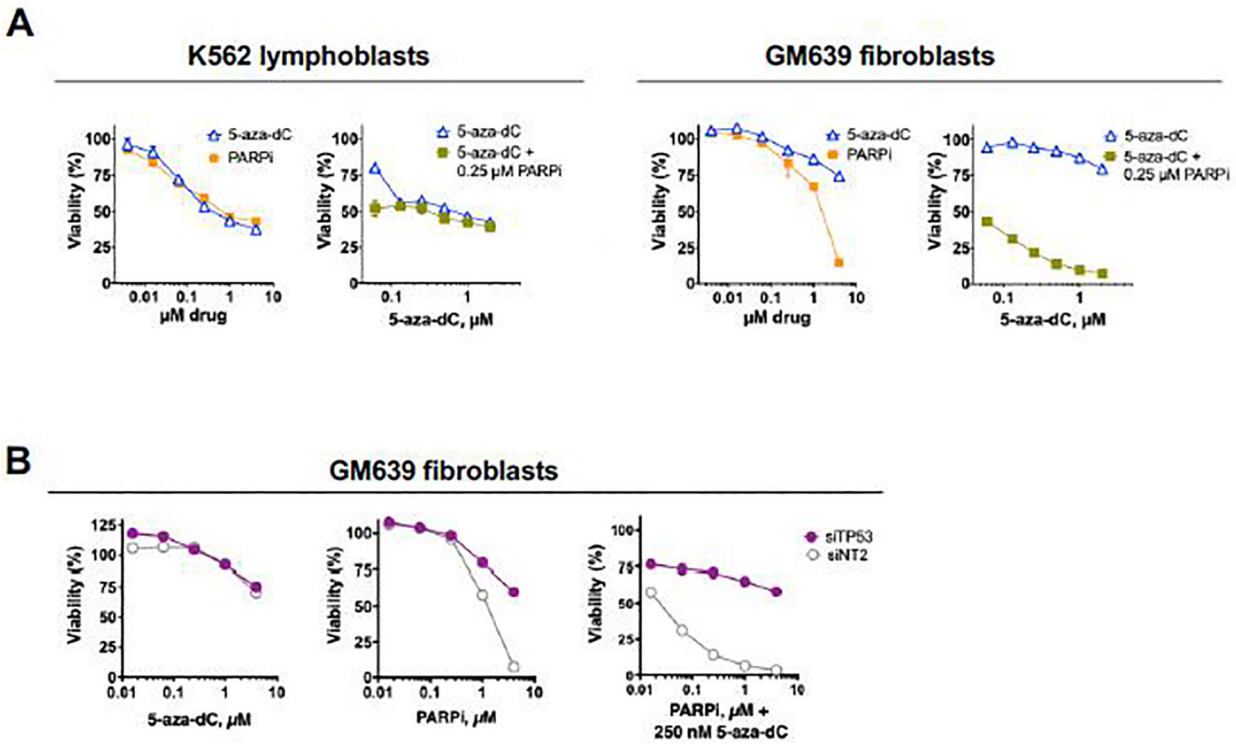

Fig. 1. Responses of K562 and GM639 cells to drug treatment

(A) Dose-response analysis of viability of K562 or GM639 cells treated for 96 hr with indicated concentrations of drug(s). Cells were incubated for 24 hr with 5-aza-dC prior to addition of PARPi. Viability assays were repeated twice, a representative experiment is shown.

(B) Effect of depletion of TP53 on the response of GM639 cells to drug treatment quantified by CellTiter-Glo viability assays. Cells were treated with 5-aza-dC, PARPi (talazoparib) or indicated combinations of PARPi and 5-aza-dC for 72 hr. Prior to drug treatment, cells were treated for 48 hr with siTP53, or non-specific siRNA, siNT2.

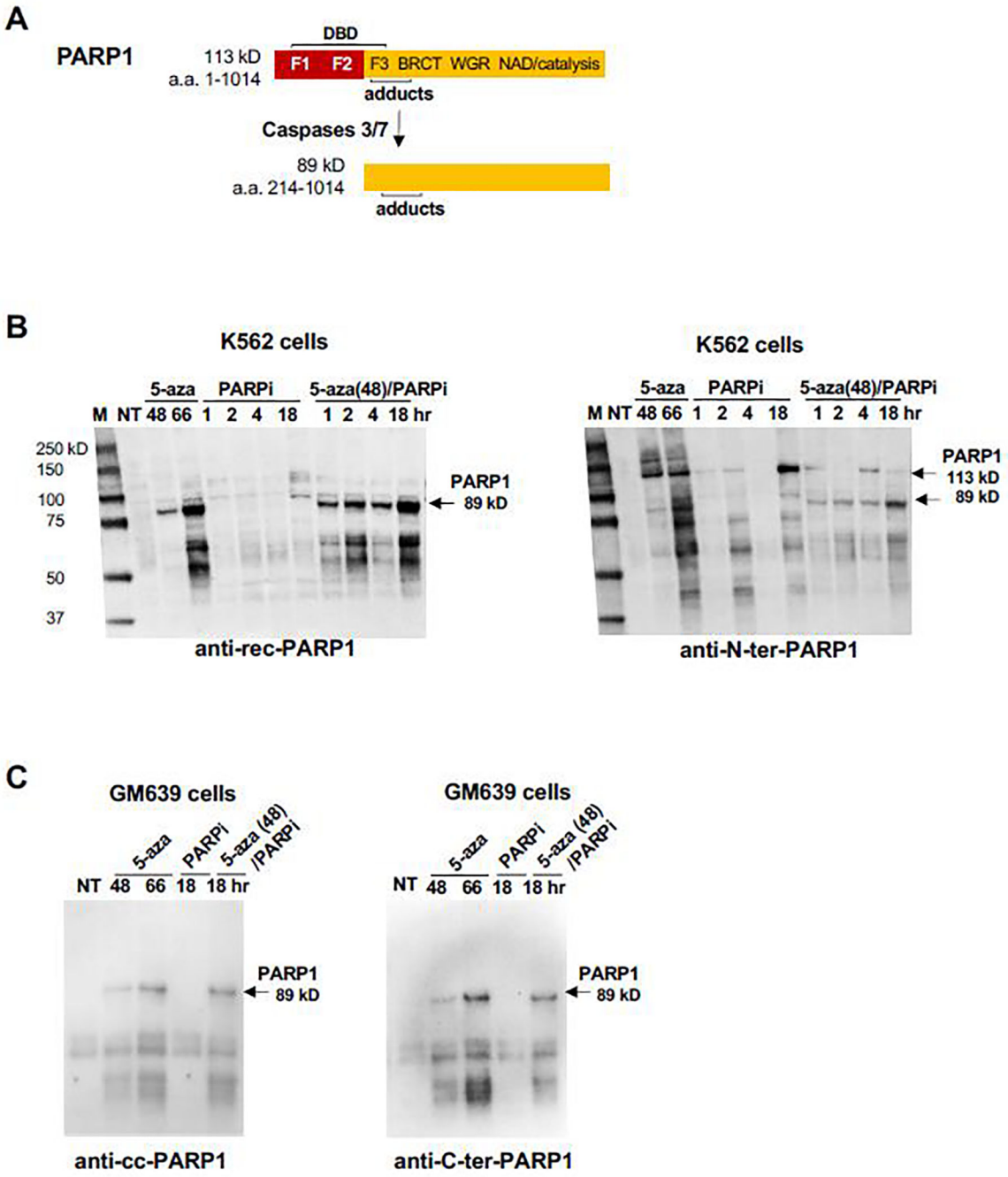

Fig. 2. RADAR/Western blots Identify PARP1-DNA Adducts Induced by 5-aza-dC

(A) PARP1 apoptotic cleavage. The 113 kD PARP1 polypeptide contains three zinc finger motifs (F1, F2 and F3) in the DNA binding domain (DBD); the BRCT, WGR and NAD binding/catalytic domains; and the region to which covalent adducts have been mapped [22]. Caspases 3/7 cleave PARP1 within the DBD, generating a 24 kD fragment (not shown) and an 89 KD fragment bearing a new N-terminal neo-epitope.

(B) Western blot analysis of PARP1-DNA adducts isolated from K562 cells, probed with (left) anti-rec-PARP1 or (right) anti-N-ter-PARP1. A single blot was washed but not stripped

between probings. Cells were treated for indicated times with 1 μM 5-aza-dC (5-aza) or1 μM BMN-673 (PARPi); or pretreated with 1 μM 5-aza-dC for 48 hr, after which PARPi was added and culture continued for indicated times. M, marker (kD); NT, untreated sample. Arrows identify 113 kD and 89 kD PA.

(C) Western blot analysis of PARP1-DNA adducts isolated from GM639 cells. Duplicate blots were probed with (left) anti-cc-PARP1 mAb or (right) anti-C-ter-PARP1 mAb. Notations as in panel B.

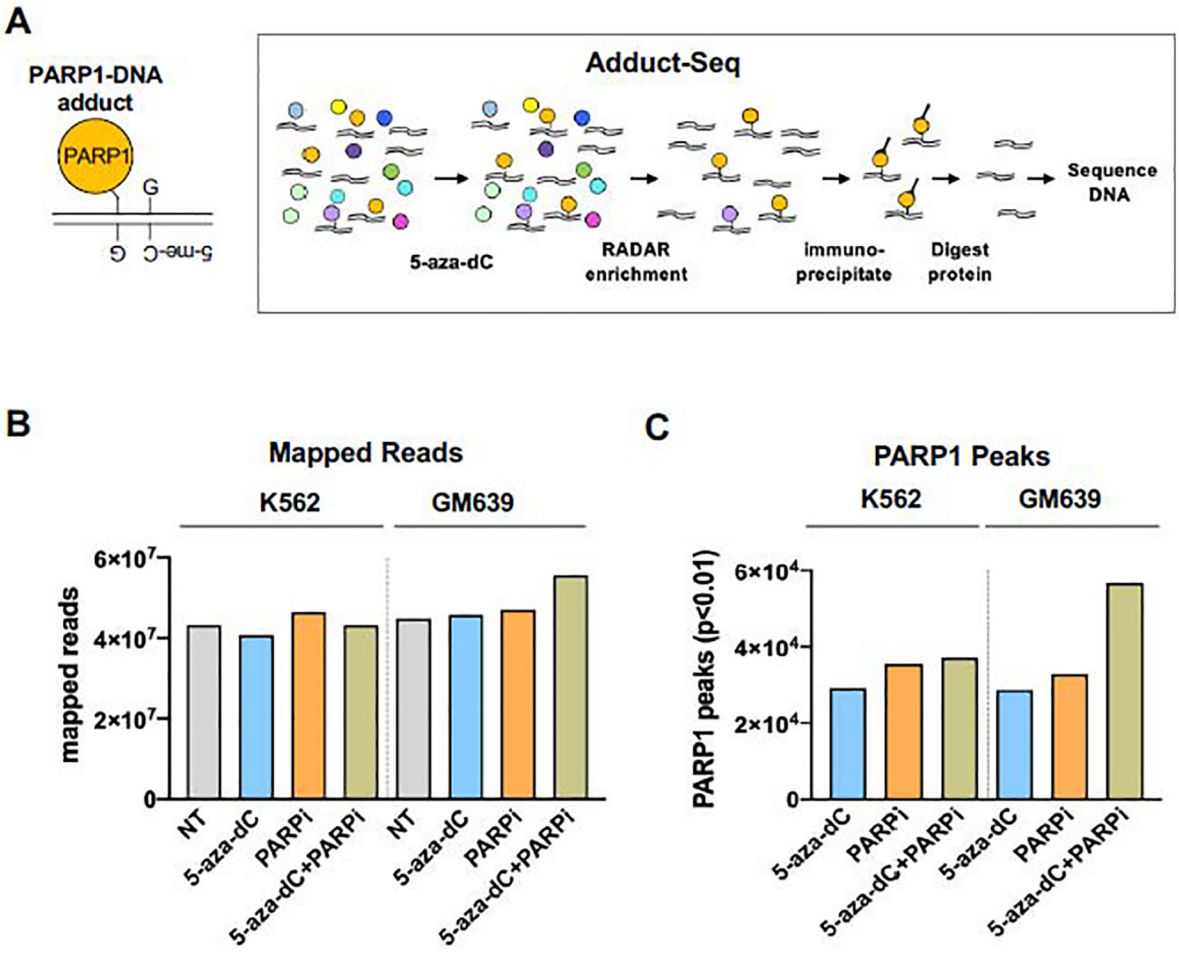

Fig. 3. Recovery of PARP1-DNA adducts by Adduct-Seq

(A) Outline of Adduct-Seq characterization of adducted DNA. Left, Predicted PARP1-DNA adduct at hemi-methylated CpG. Right, recovery of PARP1-DNA adducts; see text for details. Protein (circles), DNA (double lines).

(B) Mapped reads generated by Adduct-Seq of K562 or GM639 cells untreated (NT) or treated as indicated.

(C) PARP1 peaks identified by Adduct-Seq in K562 or GM639 cells treated as indicated.

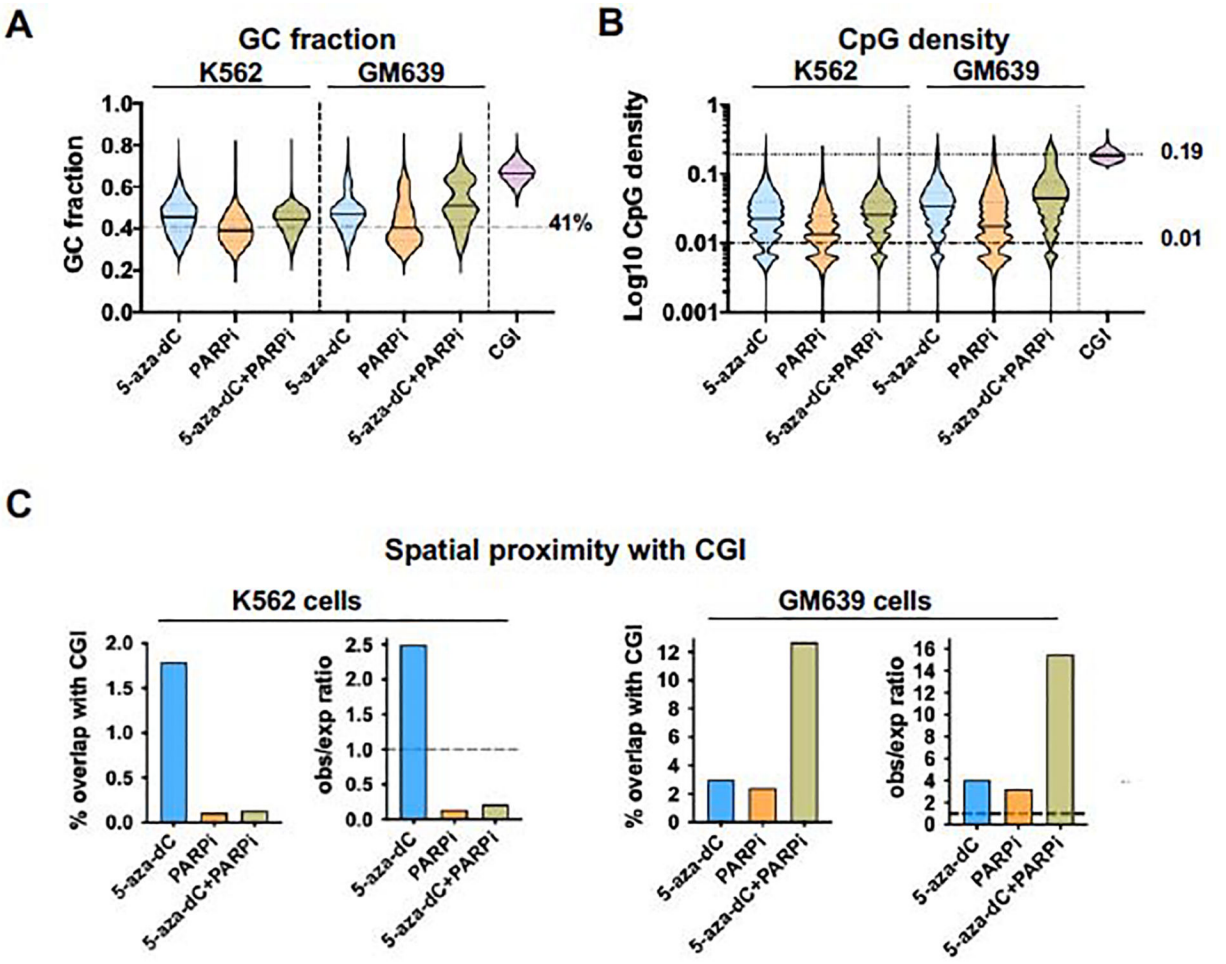

D

	K562 cells			GM639 cells		
	5-aza-dC	PARPi	5-aza-dC +PARPi	5-aza-dC	PARPi	5-aza-dC +PARPi
Relative distance test (proximity)	3.6 e-12	0.2	0.003	0	4.6 e-12	0
Projection test (overlap)	0	n/a	n/a	0	0	0

Fig. 4. Genomic features of PARP1-DNA adducts recovered from drug-treated cells

(A) Violin plots of GC fraction of adducted DNAs recovered from K562 or GM639 cells after indicated treatments. Genome average GC fraction indicated by a dashed line.

(B) Violin plots of CpG density of adducted DNAs recovered from K562 or GM639 cells after indicated treatments. Mean values of PARP1 peaks and CGI are marked by solid lines on violin plots; genomic average CpG density indicated by dashed line; mean CpG density of CGI indicated by a dotted line.

(C) Results of spatial proximity analysis of DNAs analyzed by Adduct-Seq, showing % overlap with CGI in absolute values (left) and observed/expected (obs/exp) ratios (right) for each cell type. Dashed lines, ratio = 1.

(D) Spatial correlation p-values for Adduct-Seq peaks and CGI locations shown in panel C. n/a – insufficient overlap for test to be applied.

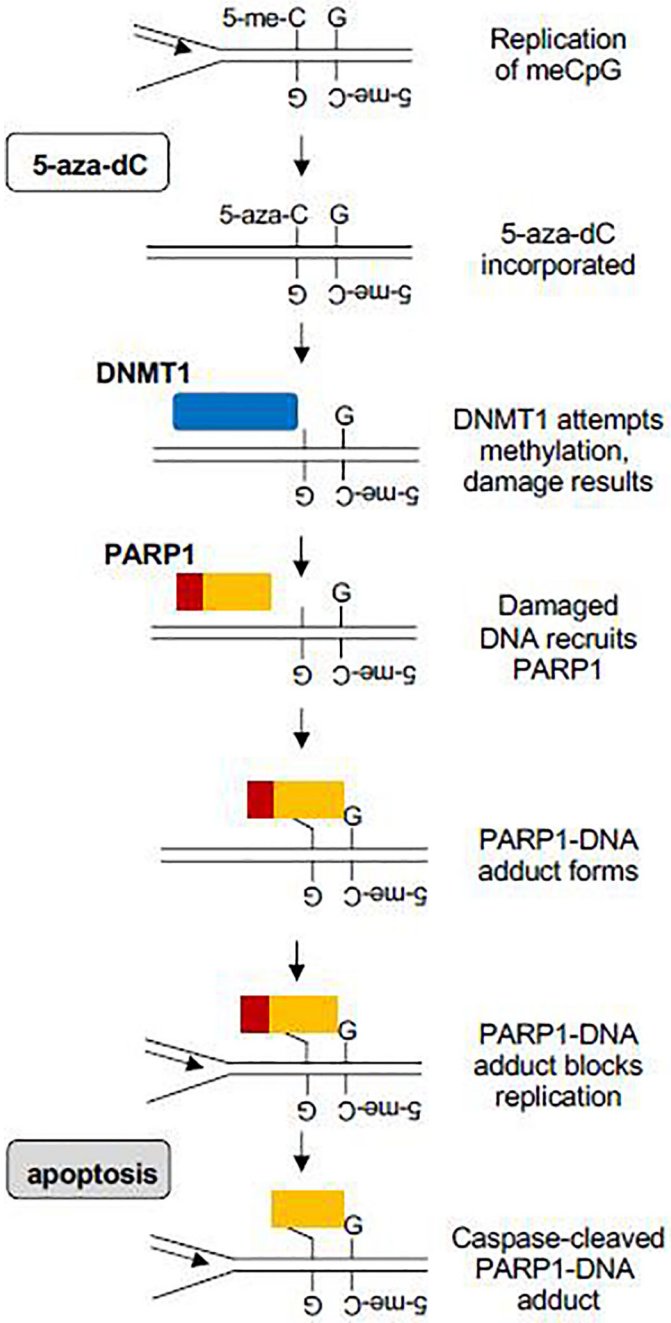

Fig. 5. Working model for induction of cytotoxic PARP1-DNA adducts by 5-aza-dC

Proliferation in the presence of 5-aza-dC results in incorporation of 5-aza-C opposite a methylated CpG dinucleotide. Thwarted DNMT1 activity at this site results in DNA damage. PARP1 is recruited to the damage, where it forms a DNA adduct that — if not repaired — may cause replication arrest and cell killing, accompanied by activation of caspase 3/7 which cleaves adducted PARP1, creating the signature N-terminal neo-epitope.